Micro and Nano Systems Letters

CORRESPONDENCE Open Access

Flexible sensing probe for the simultaneous monitoring of neurotransmitters imbalance

Hye Bin Cha[1,2], Yao Zhang[1,3], Hyun-Yong Yu[2] and Yi Jae Lee[1,4*]

Abstract

Simultaneous detection of multiple neurotransmitters and their related activities is crucial for enhancing our understanding of complex neurological mechanisms and disorders. In this study, we developed a flexible, high-sensitivity multi-electrodes array probe capable of concurrent detection of four neurotransmitters: dopamine, serotonin, acetylcholine and glutamate. The probe was fabricated on a polyimide substrate with 16 circular gold-film electrodes. These electrodes were modified with PEDOT/GluOx and PEDOT/ChOx for enzymatic detection of glutamate and acetylcholine, and with rGO/PEDOT/Nafion for the detection of dopamine and serotonin. Our electrochemical sensor achieved sensitivities of 184.21 and 219.29 μA/μM cm^2 for glutamate and acetylcholine, respectively, with limits of detection (LOD) of 0.0242 and 0.0351 μM within a concentration range of 0.1–100 μM. For dopamine and serotonin, the sensor showed sensitivities of 195.9 and 181.2 μA/μM cm^2, respectively, with LOD of 0.4743 and 0.3568 μM. This research advances the field of neurochemical sensing and provides valuable insights into the balance of neurotransmitters associated with neurological disorders. These insights improve diagnostic and therapeutic strategies.

Keywords Flexible probe, Multi-neurotransmitters, Balance monitoring, Reduced graphene oxide, PEDOT:PSS

Introduction

The complexity of the human brain and its functions depends on the delicate balance and complex interplay of various neurotransmitters. Disruptions in neurotransmitter levels may lead to numerous neurological disorders, such as Alzheimer's disease, Parkinson's disease, anxiety, and bipolar disorder. Glutamate and choline, crucial excitatory neurotransmitters, play a pivotal role in maintaining the excitatory/inhibitory (E:I) balance in the brain [1–3]. Many studies have indicated that imbalances between neurotransmitters can lead to various neurological disorders. Specifically, an imbalance between cholinergic and dopaminergic activity in the striatum is implicated in conditions such as Parkinson's disease [4–6]. Therefore, there is a need for methods to monitor and quantify neurotransmitter levels to detect and address these imbalances.

The normal levels of DA in the brain are reported to range between 0.2 and 1 μM, while 5-HT levels are documented at 0.28 to 1.14 μM [7, 8]. Glutamate and choline concentrations are described in the literature as ranging from 0.2 μM to approximately 20 and several μM, respectively [9, 10].

Current methods for neurotransmitter detection, such as high-performance liquid chromatography and mass spectrometry, have been offered high accuracy but there are some limitations, such as long detection times, high costs, complex sampling preparation, and impossible for continuous monitoring [11, 12]. These challenges necessitate the development of more efficient, cost-effective, and user-friendly techniques. Electrochemical sensing methods like differential pulse voltammetry (DPV) and

*Correspondence:
Yi Jae Lee
yijaelee@kist.re.kr
[1] Brain Science Institute, Korea Institute of Science and Technology, Seoul, Republic of Korea
[2] Department of Electrical Engineering, Korea University, Seoul, Republic of Korea
[3] Department of Mechanical Engineering, Korea University, Seoul, Republic of Korea
[4] Division of Bio-Medical Science & Technology, KIST School, University of Science & Technology (UST), Daejeon, Republic of Korea

chronoamperometry have emerged as promising alternatives due to their simplicity, rapid detection capabilities, and high accuracy for precise neurotransmitter detection.

Recent advancements in materials have introduced carbon nanomaterials, particularly graphene, as exceptional tools for enhancing the sensitivity and specificity of electrochemical biosensors [13, 14]. While chemical vapor deposition is the primary method for fabricating graphene-based devices, this approach presents significant challenges due to the complexity and difficulty of device integration, as well as graphene's poor dispersion in solvents. Carbon nanotubes (CNTs) have also garnered significant attention from electrochemists for the development of improved sensing platforms, largely because of their electrocatalytic properties, which are particularly attributed to defects on the edge planes of the CNT structure [15, 16]. Despite the availability of such materials, there remains a need for suitable materials that can selectively and efficiently detect target substances.

While significant progress has been made in developing sensitive measurement techniques for individual neurotransmitters, there remains a notable gap in the simultaneous monitoring of multiple neurotransmitters and their interactions [17]. Addressing these issues, recent research has shifted towards developing multifunctional sensors capable of concurrent detection of multiple neurotransmitters. These advancements aim to provide a more comprehensive understanding of neurological functions and disorders.

In this study, the flexible sensing probe with a multielectrode array performed simultaneous multi-neurotransmitters detection. Modified electrodes with reduced graphene oxide/PEDOT:PSS/Nafion (rGO/PP/NF) have shown significant potential in detecting DA and 5-HT with high sensitivity and selectivity. Since the graphene oxide can be deposited onto desired seed metal electrode, the electrochemically deposited graphene oxide could convert reduced graphene oxide by simple electrochemical reduction [18]. In addition, the negatively charged nature of graphene oxide helps repel negatively charged interferents like uric acid (UA) and ascorbic acid (AA), thereby increasing the selectivity of the electrode [19]. In the case of detection for choline and glutamate, the PEDOT:PSS was electroplated and the enzymes were simply immobilized on the electrodes.

In addition, monitoring the responses of 4 neurotransmitters (NTs) under induced imbalance conditions was conducted. This study not only allows for the simultaneous detection of various neurotransmitters but also offers enhanced sensitivity, selectivity, and NTs' imbalanced level monitoring capabilities. This innovative approach has expectations for advancing our understanding of neurological disorders and improving diagnostic and therapeutic strategies.

Materials and methods

Materials

For fabricating the flexible sensor configuration, Polyimide (PI, VTEC 1388) was acquired from Richard Blaine International, Inc., Philadelphia, PA, USA. DNR-L300-30 was obtained from Dongjin, Seoul, Korea. AZ 9260 was acquired from AZ Electronic Materials, NJ, USA. Phosphate buffer saline (0.1 M PBS, pH 7.4) was obtained from Duksan General Science in Korea. DA, 5-HT, glutamate, choline, agarose, choline oxidase, o-phenylenediamine, glutaraldehyde, Nafion, ascorbic acid (AA), uric acid (UA), glucose, epinephrine (EP), norepinephrine (NE) and choline oxidase (100 units) were purchased from Sigma-Aldrich for electrochemical analysis. Glutamate oxidase (25 units) was from Yamasa, Japan.

Methods

The electrochemical performances of the sensors were evaluated by an Autolab (PGSTAT 302 N, NOVA software, Ecochemie, Utrecht, The Netherlands). Three electrode configurations were used for CV, EIS with an Ag/AgCl reference, Pt counter, and modified electrode (rGO/PP/NF, PP/ChOx, PP/GluOx) as a working electrode. The detection of simultaneous NTs wasmeasured using a μStat 8000 Multi Potentiostat/Galvanostat from DropSens company. For detection of neurotransmitters, bare Au electrodes near the working electrode were used as counter and reference electrodes.

The CV with potential limits of − 0.2 and 0.8 V was performed with a scan rate of 100 mVs^{-1}, and the frequency range of EIS was from 1 to 105 Hz. The parameters of the DPV measurements were set as follows, i.e., the scan rate was 25 mV/s, the pulse width was 0.06 s, and the amplitude was 30 mV. The parameters of the amperometry measurements were set as 0.3 V. Fresh solution were prepared daily, and the sensors were kept in the dark at 4 °C to avoid the oxidation of DA. All of the experiments were conducted at ambient temperature.

The surface morphologies and elemental analyses of the electrode were evaluated respectively by scanning electron microscopy (SEM, Regulus8230).

Modification of rGO/PP/NF, PP/ChOx, and PP/GluOx surface on working electrodes

The schematic diagram of the electrodeposition procedure is displayed in Fig. 1. For preparation of rGO/PP/NF electrode, GO was electrochemically deposited (1 μA current 540 s). After deposition, the composite was dried for 3 h. The obtained GO film on the surface was then reduced to rGO. To perform these reduction processes, a

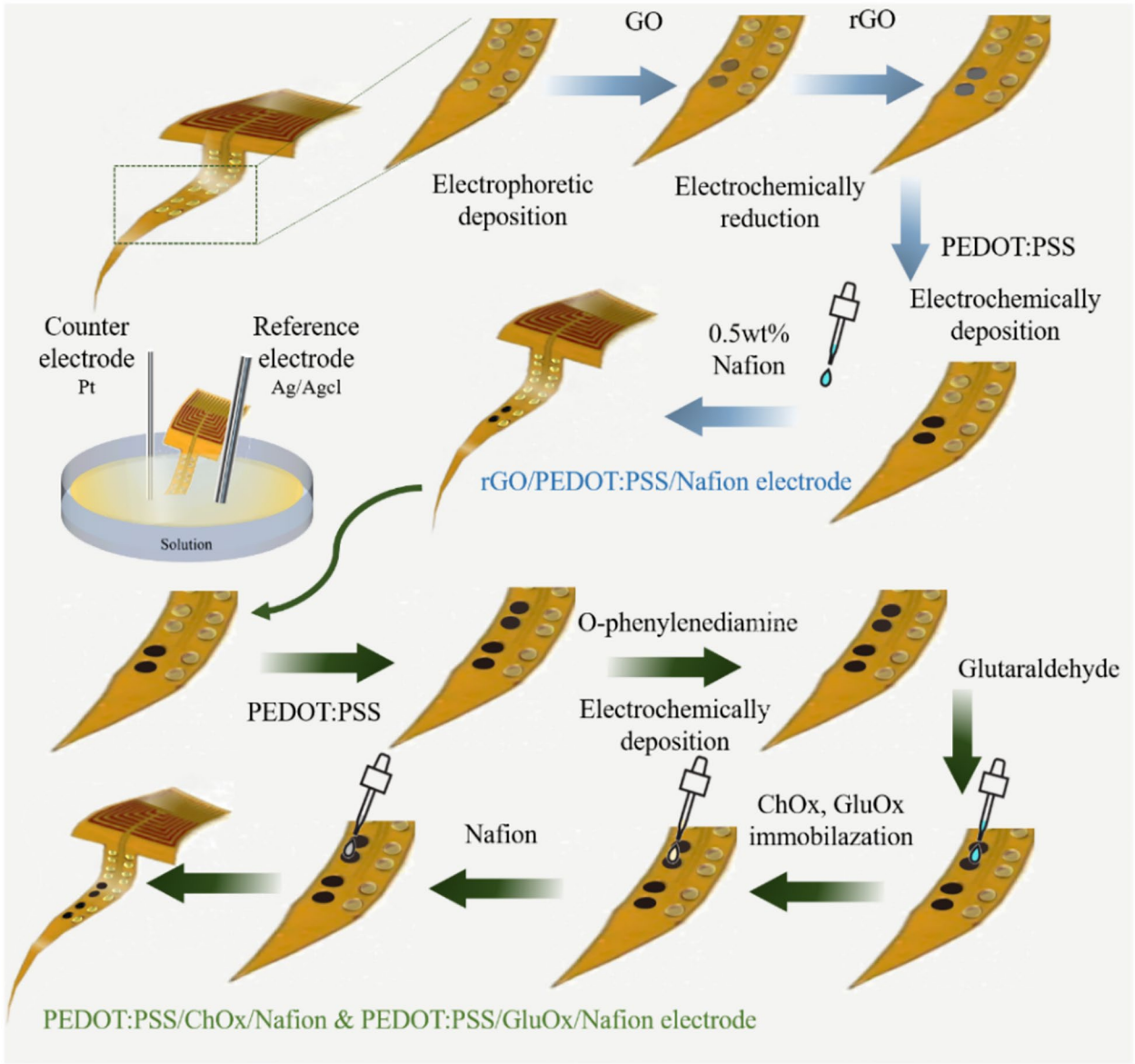

Fig. 1 Schematic drawing of preparation of the flexible sensing probe with rGO/PP/NF, PP/ChOx, and PP/GluOx electrode

cyclic voltammetry technique was applied with a potential window between 0 and − 1.5 V at a scan rate of 50 mVs^{-1} for 10 cycles in pH 4.01 buffer solution. After electrochemical reduction, the color of the rGO electrode was changed darker than GO electrode [20]. Subsequently, the electrode was electrochemically coated in PEDOT:PSS (0.01 M EDOT and 0.1 M PSS in deionized water) solution for enhanced conductivity.

Finally, the rGO/PP was coated with 0.5 wt% Nafion (1 µl) to repel unnecessary anions like AA and UA [21].

After that, for preparation of PP/ChOx and PP/GluOx electrodes, the working electrodes were electrodeposited by PEDOT:PSS. O-phenylenediamine was coated by cyclic voltammetry (0.2–0.8 V/50 mVs^{-1}/20 cycle) for protection of enzyme activity, enhancing stability and improvement of sensor [22]. The electrode was covered with 0.125 wt% Glutaraldehyde for the crosslinking between surface and enzymes [23]. Glutamate oxidase (2 µl) was drop-casted onto the electrode, enabling specific measurement of glutamate, while choline oxidase

drop-casting facilitated the measurement of choline exclusively. The modified electrodes were stored in a dark room for 24 h and the Nafion was drop casted for the protection layer of enzyme before use.

Results and discussion

Fabricated flexible sensing probe

Fig. S1. shows a simple microfabrication process of the flexible sensing probe. Initially, a polyimide (PI) layer (20 µm) was spin-coated onto a 4-inch dummy wafer. Following curing, a negative photoresist was spin-coated atop the PI layer. Subsequently, Cr/Au (10/100 nm) layers were deposited using an e-beam evaporator. After the lift-off process, a second layer of photosensitive PI was spin-coated and cured to serve as the insulation layer. A laser dicing machine was employed to trim the perimeter of the sensor. Finally, the flexible sensor was easily detached from the wafer.

Figure 2 shows the conceptual drawing, photograph image of the fabricated flexible sensing probe, and microscopy image for the rGO/PP/NF, PP/ChOx and PP/GluOx. The width of the shaft is 2.6 mm, and the length is 21.5 mm (Fig. 2a). The electrode array is composed of 16 circular electrode sites designed for multi-neurotransmitter (NT) detection, with an electrode radius of 300 µm. For detection of neurotransmitters, bare Au electrodes near the working electrode were used as counter and reference electrodes. This image depicts the optical microscope (OM) view after sequentially depositing rGO/PP/NF onto the electrodes on the probe shank (Fig. 2b). The electrode color becomes progressively darker with each deposition step from GO to rGO and then to rGO/PEDOT. The lower image shows the OM view after preparing PP/ChOx and PP/GluOx, confirming the successful attachment of the two types of enzyme particles (Fig. 2c).

Morphological analysis

Figure 3 presents SEM images of GO, rGO, rGO/PP, and rGO/PP/NF. The deposited layers of GO in Fig. 3a exhibit a single or few-layered microstructure with surface wrinkles, likely due to the presence of numerous functional groups such as hydroxyl and carboxyl groups at the edges, and carboxyl and epoxide groups within the inner structure. In Fig. 3b, the rGO electrodes display a morphology with abundant wrinkles and fluctuations. These fluctuations are crucial for maintaining the thermodynamic stability of graphene due to its 2D crystal structure. Notably, the surfaces of rGO/PP show different structures compared to rGO, appearing to be covered by uniformly distributed PEDOT:PSS (Fig. 3c). Furthermore, the surface of rGO-PP/NF appears similar with rGO/PP, with the same wrinkled structure (Fig. 3d). This suggests that the Nafion layer did not exert any significant influence on the existing layer [24]. In Fig. 3e, the pristine PEDOT:PSS layer that was polymerized onto the thin Au electrode exhibited a homogeneous distribution of the nanoparticles like grain of sand. After immobilization of enzymes, there are enzyme particles on the PEDOT:PSS surface. (Fig. 3e and f).

Electrochemical properties

To assess the electrochemical performance of the modified electrodes, we conducted measurements of interfacial impedance for Au, GO, rGO, and rGO/PEDOT:PSS electrodes in a 0.1 M PBS solution (pH 7.4), as depicted in Fig. 4a. At a frequency of 100 Hz, the recorded interfacial impedance values for Au, GO, rGO, and

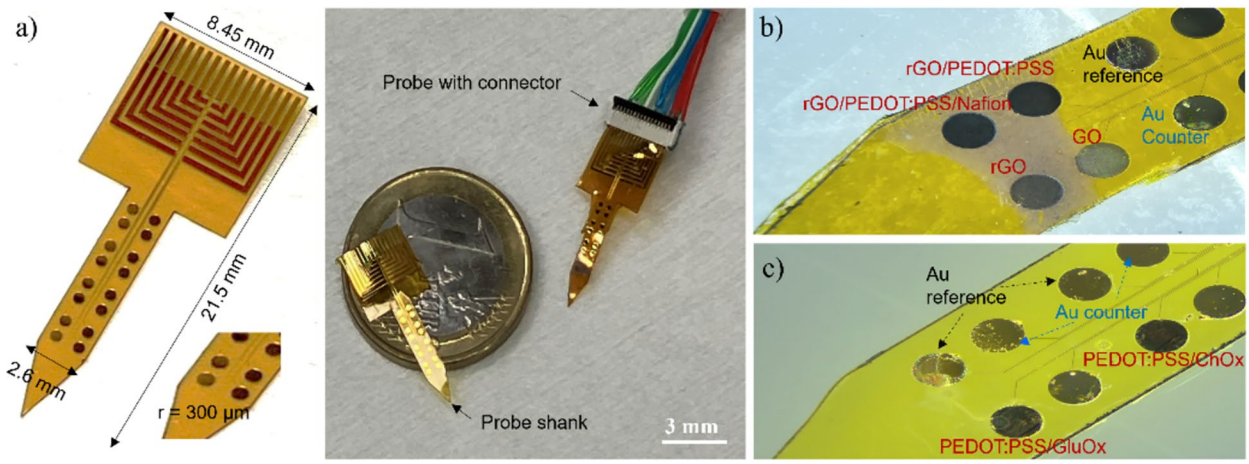

Fig. 2 **a** Microscopic image of the flexible sensing probe; **b** Photograph of the fabricated flexible sensing probe with rGO/PP/NF; **c** fabricated flexible sensing probe with PP/ChOx and PP/GluOx

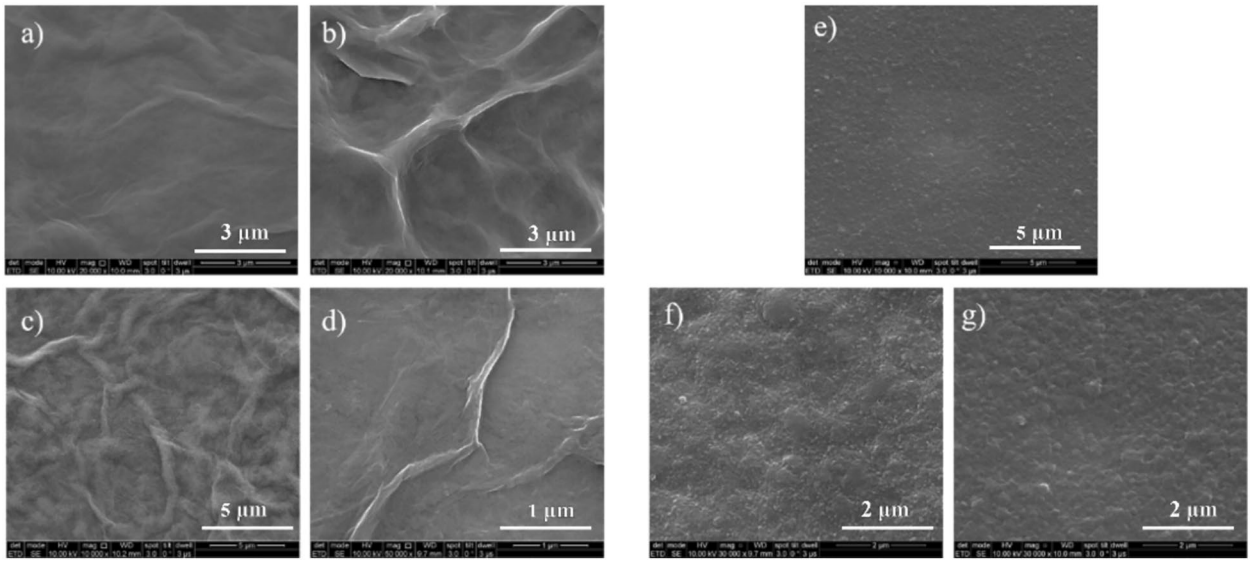

Fig. 3 SEM images of the fabricated **a** GO, **b** rGO, **c** rGO/PP, **d** rGO/PP/Nafion, **e** PEDOT:PSS, **f** PP/ChOx, and **g** PP/GluOx

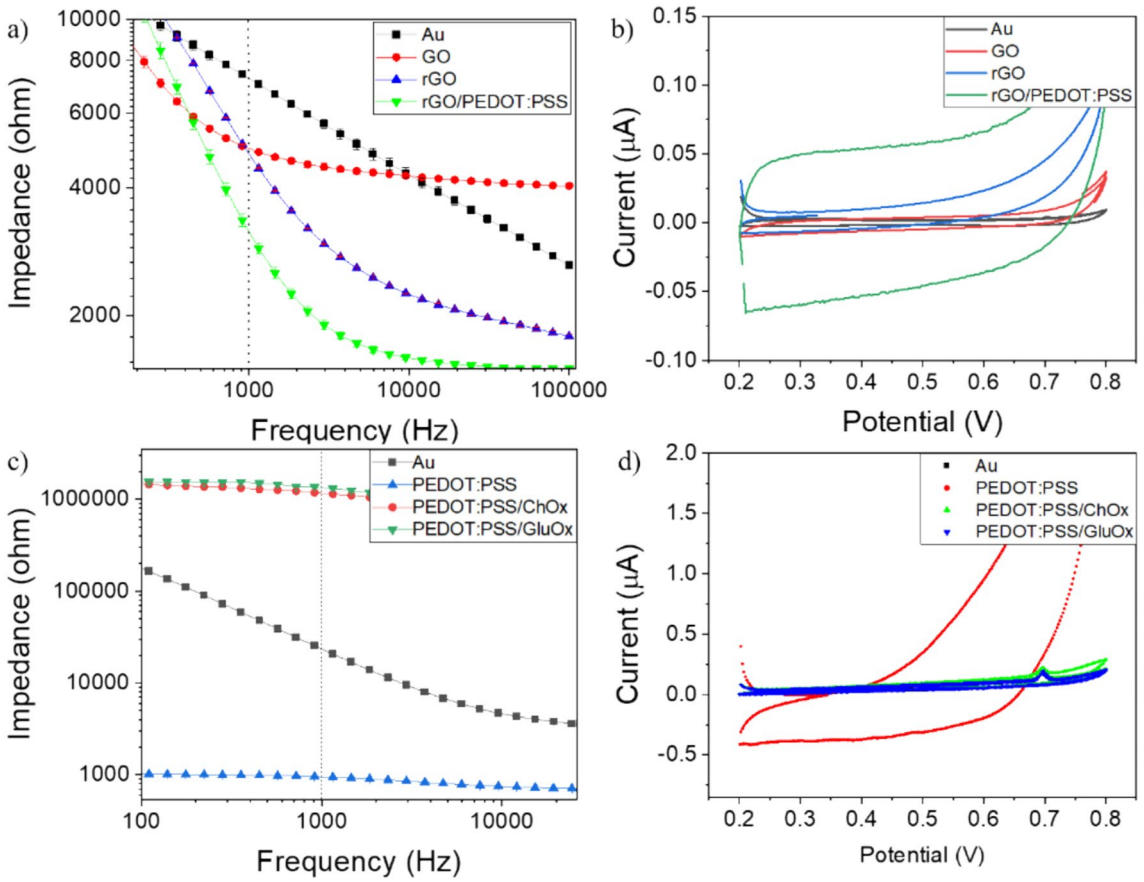

Fig. 4 Comparison of the (**a**) interfacial impedance and (**b**) cyclic voltammograms of Au, GO, rGO, and rGO/PEDOT:PSS composite; comparison of the (**c**) interfacial impedance and (**d**) cyclic voltammograms of the Au, PEDOT:PSS, PEDOT:PSS/ChOx, and PEDOT:PSS/GluOx

rGO/PP electrodes were 8826.68, 6506.12, 2066.53, and 213.613 Ω, respectively. Remarkably, the rGO/PP electrode exhibited significantly enhanced interfacial impedance compared to the other electrodes, owing to its superior conductivity and low resistance to charge transfer [24]. Additionally, after deposition of PEDOT:PSS, It showed amplified current response, indicating an augmentation of electrochemically active sites [25].

In the measured CV curve, the CSC value, representing the accumulated charges, increased sequentially in the order of Au < GO < rGO < rGO/PP, with corresponding values of 0.07, 0.925, 1.694, and 8.21 mC/cm^2, respectively (Fig. 4b).

Cyclic voltammetry measurements confirmed that the electroactive area of the electrode increased with each deposition [26]. After depositing PEDOT:PSS, the impedance decreased compared to the bare gold electrode (Fig. 4c). However, the impedance increased after immobilizing each of the choline and glutamate enzymes. This increase in impedance is likely due to the non-conductive protein shells of the enzymes, indicating that ChOx and GluOx were successfully immobilized [27].

Simultaneous detection of multi-NTs

Figure 5a shows the DPV responses to simultaneous injections of DA and 5-HT across a concentration range of 1 to 50 μM. Two distinct peaks are observed, corresponding to DA at approximately 0.2 V and 5-HT at 0.48 V. The distinct oxidation potentials of DA and 5-HT lead to their separate peaks in the DPV spectrum. The flexible sensing probe with rGO/PP/NF exhibited linear current response with increasing concentration of DA and 5-HT. The correlation coefficients for DA and 5-HT with respect to their concentrations are 0.91 and 0.98, respectively. The sensitivities for DA and 5-HT are 195.9 and 181.2 μAμM^{-1}cm^2, respectively, with limits of detection (LOD) of 0.4743 and 0.3568 μM.

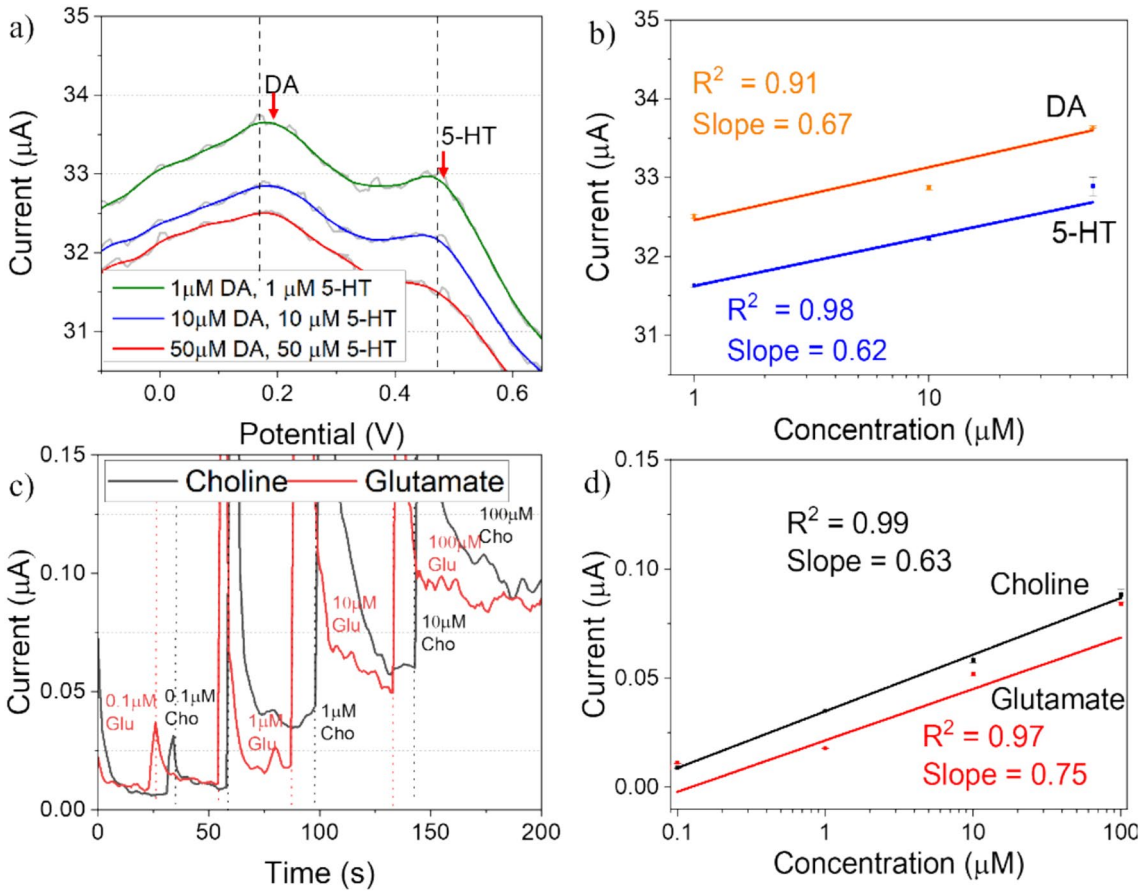

Fig. 5 **a** Simultaneous detection for DA/5-HT (DPV, 1–50 μM) at the fabricated flexible sensing probe with rGO/PP/NF; **b** Calibration curve plot of DA and 5-HT; **c** Choline/Glutamate (Amperometry, 0.1–100 μM) at the fabricated flexible sensing probe with PP/ChOx, and PP/GluOx electrodes; **d** Calibration curve plot of choline and glutamate

The amperometric current responses and calibration curve to the various choline and glutamate (0.1 to 100 μM) concentrations are shown in Fig. 5b. The correlation coefficients for choline and glutamate are 0.99 and 0.97, indicating a strong correlation between concentration and current response. The sensitivities for choline and glutamate are 184.21 and 219.29 μA μM^{-1} cm^2, respectively, with LODs of 0.0242 and 0.0351 μM.

Supplementary Fig. S2 indicates that the current responses for the four neurotransmitters are relatively well matched with individually measured ones. This result means that four different neurotransmitters can detect independently without crosstalk among them.

In order to check the response in circumstance with NT imbalance, we checked NT responses under higher concentrated conditions of the arbitrary NT (Fig. 6). All the injected NT levels were set-up based on clinically relevant concentrations found in cerebrospinal fluid [28].

In Fig. 6a, a high concentration of DA (10 μM) was injected, while other neurotransmitters were maintained at normal levels. Despite the increment of DA concentration, the responses of the other neurotransmitters remained stable, indicating their responses are independently measured. In addition, the Fig. 6b–d showed the responses to the similar circumstance. In all cases, the high concentration of arbitrary single neurotransmitter did not affect to the significant changes in the response of the other neurotransmitters. This finding demonstrates that the sensor can stably and reliably detect individual neurotransmitters even in a mixed environment.

Selectivity and stability

The presence of four types of neurotransmitters and other interfering species can lead to mixed response currents due to their closely spaced oxidation potentials. To investigate the selectivity of the rGO/PP/NF electrode, DPV was employed to measure the oxidation current response of DA at 100 μM. Glutamate (100 μM), choline (100 μM), ascorbic acid (100 μM), and uric acid (100 μM) in 0.1 M PBS (pH 7.4) were tested in Fig. 7a. The response currents in the presence of interfering substances were negligible compared to that of 100 μM DA, demonstrating the high anti-interference capability of the rGO/PP/NF to the glutamate, choline, ascorbic acid, and uric acid.

The reproducibility of the flexible sensing probe with rGO/PP/NF was investigated by using five electrodes. As depicted in Fig. 7b, the DPV-measured peak currents for DA oxidation in 0.1 M PBS (pH 7.4) were similar, ranging within ± 1.00 μA of the average value of 32.584 μA.

Figure 7c illustrates the selectivity test using the flexible sensing probe with PP/GluOx. When 100 μM of serotonin, dopamine, ascorbic acid, and uric acid were injected, no significant responses were observed. However, the sensor clearly detected 100 μM and 1000 μM of glutamate. The reproducibility of the flexible sensing probe with PP/ChOx and PP/GluOx was evaluated as shown in Fig. 7d. The current responses for 10 μM of choline and glutamate were consistent and maintained similar levels. The choline sensors showed an average current of 0.030948 μA with a variability of ± 6.71%, while the glutamate sensors exhibited an average current of 0.0283 μA with a variability of ± 6.4%. These consistent current responses across the five sensors indicate high reproducibility.

Conclusion

In this study, we successfully introduced and validated a high-sensitivity flexible sensing probe capable of simultaneously DA, 5-HT, choline, and glutamate. The sensor array, modified with rGO/PP/NF and PEDOT as working electrodes, demonstrated excellent individual NT sensing properties and reliable simultaneous detection in scenarios involving NT imbalances.

The probe's sensitivities for DA and 5-HT were 195.9 and 181.2 $\mu A \mu M^{-1} cm^2$, respectively, within a concentration range of 1–50 μM. The LOD for DA and 5-HT were 0.4743 and 0.3568 μM, respectively. For choline and glutamate, within a range of 0.1–100 μM, the probe achieved sensitivities of 184.21 and 219.29 $\mu A \mu M^{-1} cm^2$, with LODs of 0.0242 and 0.0351 μM, respectively.

The selectivity tests verified that the presence of 100 μM interferents did not significantly affect the sensor's performance, thereby ensuring reliable NT measurement. Reproducibility tests validated the probe's feasibility for use with five sensors, maintaining consistent performance over time.

0.1 M PBS is conventionally and widely used as a buffer solution in laboratory experiments due to its ability to maintain consistent pH and ionic strength, which are critical for ensuring the stability of both the sensors and the target analytes. Unlike the PBS buffer, the applicability in complex biological samples, such as extracellular fluid or brain tissue, should be further investigated about its durability, stability, and feasibility. Nevertheless, we are expecting that the developed sensing probe will be operated well even in the biological samples due to Nafion coating as a negative ion repelling and protection layer and the DPV detection technique for the selective and independent multi-NTs determination.

(See figure on next page.)

Fig. 6 Crosstalk monitoring at the simultaneous determination of the DA/5-HT and choline/glutamate to the induced imbalance situations; **a** imbalance of DA, **b** imbalance of 5-HT, **c** imbalance of choline, **d** imbalance of glutamate

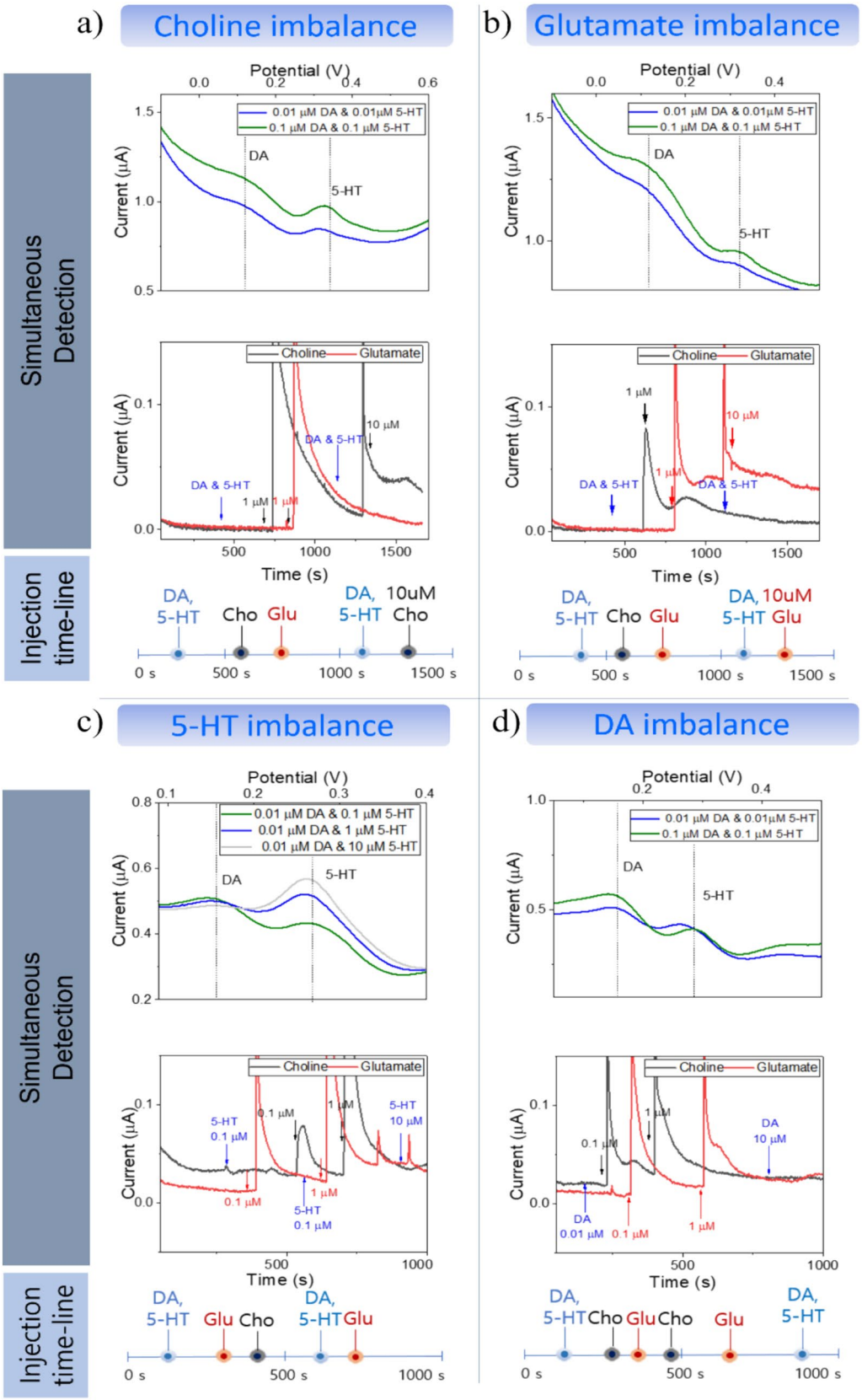

Fig. 6 (See legend on previous page.)

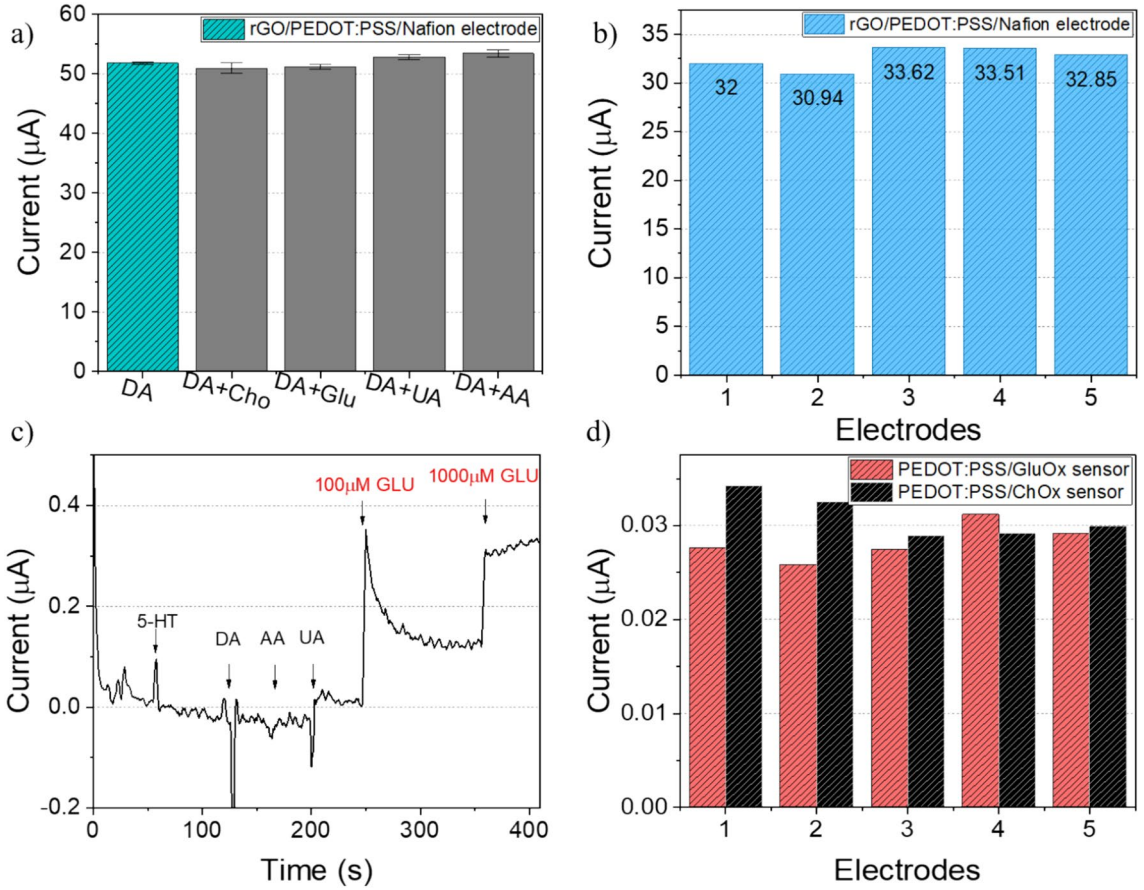

Fig. 7 Selectivity and stability of the fabricated flexible sensing probe for determination of DA/5-HT and choline/glutamate; **a** comparison of DPV responses of the DA to the adding of different interfering species (100 μM DA and 100 μM DA with interferents (100 μM Choline, Glutamate, UA, AA); **b** reproducibility of 5 different flexible sensing probe with rGO/PP/NF; **c** amperometric response of the flexible sensing probe with PP/GluOx electrode to the different interfering species (100 μM 5-HT, DA, AA, UA) and 100/1000 μM glutamate; **d** reproducibility of 5 different flexible sensing probe with PP/ChOx and PP/GluOx

This work has significant potential for applications in neuroscience research and clinical diagnostics, offering a tool for monitoring neurotransmitter dynamics with high sensitivity.

Supplementary Information

The online version contains supplementary material available at https://doi.org/10.1186/s40486-024-00211-3.

Additional file 1.

Acknowledgements
This work was partially supported by the National Research Foundation of Korea (NRF) grant (No. 2020R1C1C1004655) funded by the Ministry of Science, ICT & Future Planning of Korea government, the Technology Innovation Program (00144157, Development of Heterogeneous Multi-Sensor Micro-System Platform) funded by the Ministry of Trade, Industry & Energy (MOTIE, Korea).

Author contributions
Experiments were designed by Y.J.L. Fabrication process of the sensors was performed by Y.Z. Characterization of the flexible sensing probe were performed by H.B.C. H.B.C, H.Y.Y., and Y.J.L. wrote the main manuscript text and prepared all figures. Y.J.L. supervised all aspects of this work. All authors reviewed the manuscript and have given approval to the final version of the manuscript.

Data availability
No datasets were generated or analysed during the current study.

Declarations

Competing interests
The authors declare no competing interests.

Received: 13 August 2024 Accepted: 25 September 2024
Published online: 08 October 2024

References

1. Sarter M, Bruno JP, Parikh V (2007) Abnormal neurotransmitter release underlying behavioral and cognitive disorders: toward concepts of dynamic and function-specific dysregulation. Neuropsychopharmacology 32(7):1452–1461

2. Monday HR, Younts TJ, Castillo PE (2018) Long-term plasticity of neurotransmitter release: emerging mechanisms and contributions to brain function and disease. Annu Rev Neurosci 41:299–322
3. Kölker S (2018) Metabolism of amino acid neurotransmitters: the synaptic disorder underlying inherited metabolic diseases. J Inherit Metab Dis 41:1055–1063
4. Calabresi P, Picconi B, Parnetti L, Di Filippo M (2006) A convergent model for cognitive dysfunctions in Parkinson's disease: the critical dopamine–acetylcholine synaptic balance. Lancet Neurol 5(11):974–983
5. Velazquez R, Winslow W, Mifflin MA (2020) Choline as a prevention for Alzheimer's disease. Aging 12(3):2026
6. Xu Y, Yan J, Zhou P, Li J, Gao H, Xia Y, Wang Q (2012) Neurotransmitter receptors and cognitive dysfunction in Alzheimer's disease and Parkinson's disease. Prog Neurobiol 97(1):1–13
7. Roberts JG et al (2013) Real-time chemical measurements of dopamine release in the brain. Dopamine Methods Protoc 964:275–294
8. Siddiqi HA et al (2017) Laboratory of gastrointestinal diagnosis and pancreatic disorders. Henry's clinical diagnosis and management by laboratory methods E-Book. Elsevier Health Sciences, Amsterdam, p 306
9. Bai W, Zhou Y-G (2017) Homeostasis of the intraparenchymal-blood glutamate concentration gradient: maintenance, imbalance, and regulation. Front Mol Neurosci 10:400
10. Tayebati SK, Amenta F (2013) Choline-containing phospholipids: relevance to brain functional pathways. Clin Chem Lab Med 51(3):513–521
11. Kimmel DW, LeBlanc G, Meschievitz ME, Cliffel DE (2012) Electrochemical sensors and biosensors. Anal Chem 84(2):685–707
12. Yusoff N, Pandikumar A, Ramaraj R, Lim HN, Huang NM (2015) Gold nanoparticle based optical and electrochemical sensing of dopamine. Microchim Acta 182:2091–2114
13. Chen D, Feng H, Li J (2012) Graphene oxide: preparation, functionalization, and electrochemical applications. Chem Rev 112(11):6027–6053
14. He Y, Chen W, Gao C, Zhou J, Li X, Xie E (2013) An overview of carbon materials for flexible electrochemical capacitors. Nanoscale 5(19):8799–8820
15. Nagaki M, Konno H, Tanaike O (2010) Carbon materials for electrochemical capacitors. J Pow sour 195(24):7880–7903
16. Gu W, Yushin G (2014) Review of nanostructured carbon materials for electrochemical capacitor applications: advantages and limitations of activated carbon, carbide-derived carbon, zeolite-templated carbon, carbon aerogels, carbon nanotubes, onion-like carbon, and graphene. Wiley Interdiscip Rev Energy Environment 3(5):424–473
17. Moser I, Jobst G, Urban GA (2002) Biosensor arrays for simultaneous measurement of glucose, lactate, glutamate, and glutamine. Biosens Bioelectron 17(4):297–302
18. Zhan K, Wang W, Li F, Cao J, Liu J, Yang Z, Wang Z, Zhao B (2023) Microstructure and properties of graphene oxide reinforced copper-matrix composite foils fabricated by ultrasonic assisted electrodeposition. Mater Sci Eng, A 872:144995
19. Ko SH, Kim SW, Lee SH, Lee YJ (2023) Electrodeposited reduced graphene oxide-PEDOT: PSS/Nafion hybrid interface for the simultaneous determination of dopamine and serotonin. Sci Rep 13(1):20274
20. Liu G, Chen X, Liu J, Liu C, Xu J, Jiang Q, Jia Y, Jiang F, Duan X, Liu P (2021) Fabrication of PEDOT: PSS/rGO fibers with high flexibility and electrochemical performance for supercapacitors. Electrochim Acta 365:137363
21. Xu Z, Zhang M-Q, Zou H-Q, Liu J-S, Wang D-Z, Wang J, Wang L-D (2019) Non-enzymatic electrochemical detection of uric acid with electrodeposited Nafion film. J Electroanal Chem 841:129–134
22. Mathivanan D, Tammina SK, Wang X, Yang Y (2020) Dual emission carbon dots as enzyme mimics and fluorescent probes for the determination of o-phenylenediamine and hydrogen peroxide. Microchim Acta 187:1–9
23. Migneault I, Dartiguenave C, Bertrand MJ, Waldron KC (2004) Glutaraldehyde: behavior in aqueous solution, reaction with proteins, and application to enzyme crosslinking. Biotechniques 37(5):790–802
24. Zhang X, Zhang D, Chen Y, Sun X, Ma Y (2012) Electrochemical reduction of graphene oxide films: preparation, characterization and their electrochemical properties. Chin Sci Bull 57:3045–3050
25. Baruah B, Kumar A, Umapathy G, Ojha S (2019) Enhanced electrocatalytic activity of ion implanted rGO/PEDOT: PSS hybrid nanocomposites towards methanol electro-oxidation in direct methanol fuel cells. J Electroanal Chem 840:35–51
26. Jiwanti PK, Sukardi DKA, Sari AP, Tomisaki M, Wafiroh S, Hartati S, Wong YH, Woi PM, Juan JC (2024) Fabrication and characterization of rGO-SnO2 nanocomposite for electrochemical sensor of ciprofloxacin. Sens Int 5:100276
27. Bi R, Ma X, Miao K, Ma P, Wang Q (2023) Enzymatic biosensor based on dendritic gold nanostructure and enzyme precipitation coating for glucose sensing and detection. Enzyme Microb Technol 162:110132
28. Tschirner SK, Gutzki F, Schneider EH, Seifert R, Kaever V (2016) Neurotransmitter and their metabolite concentrations in different areas of the HPRT knockout mouse brain. J Neurol Sci 365:169–174

Publisher's Note